Nuclear-Targeted TAT-PZLL-D3 Co-Delivery DOX and p53 for Chemotherapy Resistance of SCLC

Dan Wang
Guangdong Medical University
Tianshou Cao
Guangdong Medical University
Wanyu Li
Guangdong Medical University
Li Li
Guangdong Medical University
Qunfa Huang
Guangdong Medical University
Huiling Yang
Guangdong Medical University
Hua Chen
Maoming People's Hospital
jiantao lin (linjt326@163.com)
Guangdong Medical University

Nano Express

Keywords: TAT, nucleus-targeted, small cell lung cancer, co-delivery

Posted Date: March 18th, 2021

DOI: https://doi.org/10.21203/rs.3.rs-309656/v1

Abstract

Small cell lung cancer (SCLC) accounts for 13% ~ 15% of lung cancer. It is a subtype with high malignancy and poor prognosis. Almost all patients with SCLC will inevitably have drug resistance and tumor recurrence, which has become an urgent problem in the treatment of SCLC. Nuclear-targeted drug delivery system, which enables intra-nuclear release of anticancer drugs, is expected to address this challenge. In this study, based on transactivator of transcription (TAT)'s active transport property to the nucleus, we developed a high-efficiency nucleus-targeted co-delivery vector that delivers genes and drugs directly into the nucleus of A549 cells. The system is based on a poly-(*N*-ε-carbobenzyloxy-L-lysine) (PZLL) and dendritic polyamidoamine (PAMAM) block copolymer (PZLL-D3) with TAT modified on the surface of carrier. In vitro studies showed that DOX and p53 could can be effectively transported to the nucleus and kill the cancer cells. Thus, such deliver system would bypass the drug resistance and tumor recurrence problem.

1. Introduction

Small cell lung cancer (SCLC) originated from bronchial neuroendocrine cells and belongs to a special type of bronchogenic carcinoma. Due to the occurrence of drug resistance, especially the emergence of multidrug resistance, chemotherapy failure and disease recurrence or progress. Therefore, breaking through the barriers of chemotherapy resistance of SCLC patients and improving the effect of chemotherapy is a common concern in the field of treatment at this stage. It can be detected in SCLC tissues and SCLC cell lines cultured in vitro that the high expression of P-glycoprotein. It can block the process of alkylating agents such as doxorubicin (DOX) from entering the nucleus and play an intermediate gate effect. After that, the drugs are discharged from the cells through the mechanism of exocytosis, resulting in the decrease of drug concentration in the cells and the formation of drug resistance. Therefore, it is possible to solve the problem of drug resistance of SCLC if DOX can be directly transferred into the nucleus by vector. Besides chemotherapy, gene therapy is another important treatment for SCLC. Whether it is chemotherapy or gene therapy, the nucleus plays an important role. In fact, the nucleus is the most important organelle in the cell, because it is the central hub of the cell. The cell preserves and transcribes the genetic information in the nucleus. At the same time, it is also the place where many therapeutic drugs work effectively. Usually, the goal of gene therapy is to correct functional genes by transferring therapeutic genes into the nucleus [1]. However, due to the existence of many biological barriers, it is hard for free anticancer drugs / DNA to maintain their activity after reaching the nucleus [2]. So, construction of a nuclear targeting vector is expected to markedly improve the anticancer efficiency of existing drugs, so it is of great significance. Some nuclear targeted drug transport systems have been reported [3], such as surface modified MSNs [4] and the cell penetrating peptides (CPPs) [5]. It is well known that TAT peptides, derived from the transactivator of transcription of human immunodeficiency virus type 1 (HIV-1), are the most frequently used cell nucleus-targeting peptides [6]. Because it can be recognized by the nuclear pore complex, the carrier modified by Tat can transport all kinds of goods to the nucleus accurately [7-13].

In our former work, a cationic micelle based on a poly-(*N*-ε-carbobenzyloxy- L-lysine) (PZLL) and dendritic polyamidoamine (PAMAM) block copolymer (PZLL-D3) has been synthesise and used for co-delivery of doxorubicin (DOX) and DNA [13]. In this work, we constructed a cationic micelle, in which TAT was modified on the surface of PZLL-D3 as a nuclear targeting molecule. DOX and p53 were loaded for reversing SCLC resistance of A549 cells. The crux of the matter in this work is could DOX and p53 be transported to the nucleus smoothly and efficiently by TAT-PZLL-D3. To prove this, a nucleus-targeted assay has been executed.

2. Materials And Methods

2.1. Materials

Poly-(*N*-ε-carbobenzyloxy-L-lysine) (PZLL) and dendritic polyamidoamine (PAMAM) block copolymer (PZLL-D3) were synthesized in our laboratory. Ethanediamine, methyl acrylate, cystamine and DOX were purchased from Aladdin (China). TAT(YGRKKRRQRRRC[NH2]), plasmid p53 were purchased from Invitrogen (Carlsbad, CA).

2.2 Synthesis

2.2.1 Synthesis of TAT-PZLL-D3 (Figure 1)

PZLL-D3 was synthesized like our former work reported [13].

Synthesis of Mal-PZLL-D3: First, N-Maleoyl-β-alanine (10 mmol) was solubilized in 20 mL of DCM, one drop of DMF was added later with 2 mL of thionyl chloride as catalyst. The reaction was kept stirring at room temperature for 24 h. Next, the excess solvent was removed by vacuum and the white powder N-[2-(Chloroformyl)ethyl] maleimide was obtained.

N-[2-(Chloroformyl)ethyl] maleimide (5mmol) was solubilized in 50 mL DCM, then 100 mL DCM with PZLL-D3 (1mmol) and TEA (1mmol) was added. The reaction was kept stirring at 0°C for 4h, and then the temperature rise to room temperature for another 12h. After the reaction, the solvent was removed by vacuum drying. The white powder was dispersed in 5ml water and then dialyzed with water for 24 hours. Mal-PZLL-D3 (yield 63%) was obtained by lyophilization.

Synthesis of TAT-PZLL-D3: Mal-PZLL-D3 (1 mmol) and TAT (1.2 mmol) were solubilized in 10 mL of pH 7.4 PBS buffer, and react for 24h in darkness. The reaction solution was sealed in a dialysis bag and dialyzed against pH 7.4 PBS for 24h. The solution was then freeze-dried to obtained TAT-PZLL-D3 (87%).

2.3 Cellular uptake and intracellular distribution.

2×10^5 A549 cells were seeded into confocal dish. After 24h, cells were incubated with FITC-labeled PZLL-D3 or TAT-PZLL-D3 for 2h. Confocal dishs were then washed with PBS twice and stained with DAPI for

nuclear staining. The spread of the fluorescence in tumor cells was recorded by a Leica Microsystem (SP8, Leica, Germany).

2.4 Drug loading and release

To prepare DOX-loaded micelles,10 mg TAT-PZLL-D3 and 5.0 mg of DOX were mixed and dissolved in 5.0 mL DMSO solution. To load DOX in the carrier, the solution was transfered to a dialysis tube and dialyzed against water for TAT-PZLL-D3 self assembly to form micelles; After loading, the solution was screened with a 0.45μm filter and lyophilized. Free DOX solution was gathered and measured by a UV-3200 spectrophotometer at 488 nm. The loading efficiency of DOX in TAT-PZLL-D3 was calculated as follows:

$$\text{Loading Efficiency} = \frac{(\text{DOX before loading} - \text{DOX without loading})}{\text{DOX before loading}} \times 100\%$$

The DOX-release experiments were performed at 37 ℃. Briefly, DOX/TAT- PZLL-D3 samples were put in a dialysis tube and incubated in 20mL of PBS. Data was collected every 2 h. At settled schedule, 2mL of release solution was collected and deceted.

2.5 In vitro DOX transfer efficiency

Briefly, prior to observation, 2×10^5 A549 cells were cultured in 6-well plates. Cells were then incubated with DOX/PZLL-D3 or DOX/TAT-PZLL-D3 samples for 6h 24h later. Cells were then washed with PBS and the nucleus was stained by DAPI. The spread of the fluorescence in A549 cells was recorded by a Leica Microsystem (SP8, Leica, Germany). In another group, cells were trypsinized and collected, flow cytometry analysis was performed by a flow cytometer (BD Biosciences, USA) for DOX fluorescence expression.

2.6 Apoptosis and MTT assay

Apoptosis test was carried out as follow: A549 cells were seeded in a 24-well plates. Cells were then incubated with TAT-PZLL-D3, PZLL-D3/p53/DOX or TAT-PZLL-D3/p53/DOX complexes at 37 ℃ for 24 h. Further, the cells were gathered and tested by an Annexin V-FITC/PI apoptosis detection kit by a flow cytometer (BD Biosciences, USA).

Cell viability was detected using MTT method. A549 cells were seeded in 96-well plates and incubated for 24h. Further, cells were treated by TAT-PZLL-D3, PZLL-D3/p53/DOX or TAT-PZLL-D3/p53/DOX, then co-cultured for 24h to assess the in vitro cell viability of the designed prescription.

3. Results And Discussion

As display in the Fig.2, the peak of Mal-PZLL-D3 at 7.0-7.4 ppm could assigned to characteristic peaks on benzene ring of PZLL-D3, the peak at 7.5 ppm could assigned to characteristic peaks on triazole ring after click reaction, the double peak at 6.3 ppm could assigned the double bonds in the maleimide group, the peak at 2.4-2.8 ppm could assigned to characteristic peaks of D3. Different with Mal-PZLL-D3, the peak

of TAT-PZLL-D3 at 6.4 ppm has vanished, which owing to the click reaction between TAT and double bonds of maleimide group. The result means TAT attached to the PZLL-D3 smoothly.

To evaluated cellular uptake of PZLL-D3 and TAT-PZLL-D3, they were cultured with A549 cells and recorded by CLSM. As the Fig.3 showed, there was very few PZLL-D3 in the nuclei after 6 h, on the contrary, it can be clearly seen in nuclei of A549 cells after co-cultured with TAT-PZLL-D3 for 6 h, as displayed by the green fluorescence from FITC lighting up the nuclei. It could be drawn from the result that the nuclear targeting ability of the carrier is obviously enhanced by the modification of TAT.

Many polycationic gene vectors have buffer capacity below physiological pH, such as polyamide, polyethyleneimine (PEI) and so on, they are very effective gene transfer reagents. Especially branched PEI, The ratio of primary amino group, secondary amino group and tertiary amino group is 1:2:1 in the molecule. These widely existing amino groups make PEI has buffering capacity in the whole physiological pH range [14]. This unique property enables PEI to overcome the degradation of acid endosomes and lysosomes through the "proton sponge effect", so as to obtain higher transfection efficiency. Therefore, the buffer capacity of polymers at physiological pH, especially in the range of 5.1 to 7.4, is of great significance for breaking through the endosome barrier during transfection. Compared with NaCl solution, PZLL-D3 has obvious buffer capacity (Fig. 4A), which could be owe to the presence of abundant tertiary amino groups from the conjugated D3 dendrons. Its buffering capacity for acidic environment makes the pH value of solution decrease slowly with the increase of hydrochloric acid volume, instead of rapid pH change like that of NaCl solution. After the modification of TAT, its buffering capacity decreased slightly, which may be due to the reduction of the number of amino groups on D3 surface.

The shape and size of particles are important factors affecting their entry into cells. TEM results(Fig.4B) showed that TAT-PZLL-D3/p53 formed spherical particles with a diameter of about 200 nm, which was favorable for the accumulation at tumor site and less recognizable from the RES with a consequent longer blood circulation [15]. The shape and size of the particles were favorable for endocytosis. The zeta potential measurement shows that the particle size is about 200 nm, which is consistent with the results of TEM (Fig. 4C). Figure 4 shows the cumulative release curve of DOX from TAT-PZLL-D3/p53/ DOX. The results show that the cumulative release rate of DOX is 40% within 24 hours, then it enters the slow release period, and rises to 60% after 48 hours. This is similar to our previous results [16], indicating that the DOX release from the core will not be affected by the recombination of p53 plasmid and the modification of TAT.

Since the target of DOX is the nucleus, how to deliver DOX to its target nucleus accurately and quickly is the key to realize the efficacy of DOX. For this reason, we observed the ability of TAT-PZLL-D3/DOX and PZLL-D3/DOX to enter nucleus after being absorbed by A549 cells through CLSM and flow cytometry. As shown in Fig.5A, both TAT-PZLL-D3/DOX and PZLL-D3/DOX could be absorbed by cells after being co cultured with cells for 6h. However, the results showed that the red fluorescence of DOX carried by TAT-PZLL-D3 coincided well with the blue fluorescence of nucleus after endocytosis, indicating that TAT-PZLL-

D3 could effectively deliver DOX to the nucleus after 6 hours of co-culture with tumor cells, more importantly, the red fluorescence of TAT-PZLL-D3 group was stronger than in the PZLL-D3 group, flow cytometry showed DOX-positive cell population of TAT-PZLL-D3 was 57.6%, higher than 31.8% of PZLL-D3 (Fig.5B). For the nuclear transport typically depend on specific channels [17], the cellular uptake result showed that after surface of the carrier was modified with TAT, DOX can be effectively transfer to the nucleus of A549 cells.

To confirm the transfection effect of p53, the expression quantity of p53 protein was tested by western blot. Figure 6 displayed TAT-PZLL-D3/p53 led to higher p53 protein expression than TAT-PZLL-D3 and PZLL-D3/p53.The apoptosis results were obtained by a FITC-labeled Annexin V/propidium iodide (PI) double-staining assay. The control group(TAT-PZLL-D3) displayed a negligible toxicity, the apoptosis rate is very low. Pretreatment with PZLL-D3/p53/DOX and TAT-PZLL-D3/p53/DOX, cause apoptosis rate increase to 23.6% and 55.4%, respectively. Compare with PZLL-D3/p53/DOX, apoptosis rate of TAT-PZLL-D3/p53/DOX risen by 31.8%, this might be due to the modification of on the surface of PZLL-D3, which lead to more p53 and DOX get into the nucleus of A549 cells. High apoptosis will lead to low cell viability. To verify our thoughts, a cell viability assessment has been carried out. As display in Fig. 8, the TAT-PZLL-D3/p53/DOX display enhanced cytotoxicity when contrast to TAT-PZLL-D3 and PZLL-D3/p53/DOX, as illustrated by their cell viability values of 38.3, 98.6 and 52.3 respectively. TAT-PZLL-D3 showed negligible cytotoxicity. PZLL-D3/p53/DOX showed less cytotoxic to A549 cells when compare with TAT-PZLL-D3/p53/DOX. Because when DOX and p53 was delivered by PZLL-D3, DOX and p53 could not deliver to the cell nucleus, DOX and p53 might be recognized by P-gp on the cell membrane and pumped out. TAT-PZLL-D3/p53/DOX cause higher cytotoxicity in A549 cells than PZLL-D3/p53/DOX due to the improved intra-nuclear delivery of p53 and DOX regulated by TAT, bypassing the drug efflux pump.

4. Conclusion

In conclusion, a nucleus-targeted cationic micelle has been developed for transfering DOX and p53 to nucleus of A549 cells. CLSM studies revealed the advantage of this nuclear-uptake cationic micelle vector. By using TAT-PZLL-D3, more DOX and p53 can efficiently go through the cell membrane and accumulated in the nuclei of A549 cells. This TAT-PZLL-D3 deliver system might offer insight into an alternative new strategy to design co-delivery vector for against chemo-resistance SCLC.

Declarations

Acknowledgments

This work was financially supported by the Foundation of Guangdong Natural Science(2020A1515010839, 2018A030313084), Foundation of South China Sea for R&D Marine Biomedicine Resources (2HC18014, 2HC18015), Foundation of Guangdong Medical University (4SG20128G,4SG20124G), Foundation of Guangdong Medical Science (B2019098, B2019222), Foundation of scientific research projects of traditional Chinese medicine of Guangdong Provincial

Bureau of traditional Chinese Medicine (20201181, 20191187) , Foundation of Guangdong Medical University (GDMUZ201806, GDMUZ2020005), Foundation of Maoming Science and Technology Plan (mmjk2020018) and Foundation of High-level Hospital Construction Research Project of Maoming People' s Hospital (ZX2020003).

References

1. Aa MAEMA, Mastrobattista E, Oosting RS, Hennink WE, Koning GA, Crommelin DJA (2006) The nuclear pore complex: The gateway to successful nonviral gene delivery. Pharm Res 23:447-459.
2. Mizutani H, Tada-Oikawa S, Hiraku Y, Kojima M, Kawanishi S (2005) Mechanism of apoptosis induced by doxorubicin through the generation of hydrogen peroxide. Life Sci 76:1439-1453.
3. Pan L, Liu J, Shi J (2018) Cancer cell nucleus-targeting nanocomposites for advanced tumor therapeutics.Chem Soc Rev 47:6930-6946.
4. Pan L, HeQ, Liu J, Chen Y, Ma M, Zhang L, Shi J (2012) Nuclear-targeted drug delivery of TAT peptide-conjugated monodisperse mesoporous silica nanoparticles.J Am Chem Soc 134:5722-5725.
5. Melikov K, Chernomordik LV (2005) Arginine-rich cell penetrating peptides: from endosomal uptake to nuclear delivery.Cell Mol Life Sci 62:2739-2749.
6. Jeang KT, Xiao H, Rich EA (1999) Multifaceted activities of the HIV-1 transactivator of transcription.Tat J Biol Chem 274:28837-28840.
7. Misra R, Das M, Sahoo BS, Sahoo SK (2014) Reversal of multidrug resistance in vitro by co-delivery of MDR1 targeting siRNA and doxorubicin using a novel cationic poly(lactide-co-glycolide) nanoformulation. Int J Pharm 475:372-384.
8. Deng ZJ, Morton SW, Ben-Akiva E, Dreaden EC, Shopsowitz KE, Hammond P (2013) T Layer-by-layer nanoparticles for systemic codelivery of an anticancer drug and siRNA for potential triple-negative breast cancer treatment.ACS Nano 7:9571-9584.
9. Wei W, Lv PP, Chen XM, Yue ZG, MaGH (2013) Codelivery of mTERT siRNA and paclitaxel by chitosan-based nanoparticles promoted synergistic tumor suppression. Biomaterials 34:3912–3923.
10. Zhao D, Liu CJ, Zhuo RX, Cheng SX (2012) Alginate/$CaCO_3$ hybrid nanoparticles for efficient codelivery of antitumor gene and drug. Mol Pharm 9: 2887-2893.
11. Zhou X, Zheng Q, Wang C, Xu J, Wu JP, Kirk TB, Ma D, Xue W J (2016) Star-shaped amphiphilic hyperbranched polyglycerol conjugated with dendritic poly(l-lysine) for the codelivery of docetaxel and MMP-9 siRNA in cancer therapy.ACS Appl Mater Interfaces 8:12609-12619.
12. Lin JT, Zou Y, Wang C, Zhong YC, Zhao Y, Zhu HE, Wang GH, Zhang LM, Zheng XB (2014) Cationic micellar nanoparticles for DNA and doxorubicin co-delivery.Mater Sci Eng C 44:430–439.
13. Lin JT, Wang GH, Yang HK, Zhang DW, Zhang LM, Zhao Y (2015) Codelivery of doxorubicin and p53 by biodegradable micellar carriers based on chitosan derivatives.RSC Adv 5:105901–105907.
14. Lin JT, Wang GH, Yang HK, Zhang DW, Zhang LM, Zhao Y (2005) Exploring polyethylenimine-mediated DNA transfection and the proton sponge hypothesis.RSC Adv 7:657-663.

15. Moghimi SM, Hunter AC, Murray JC (2001) Long-circulating and target-specific nanoparticles: theory to practice.Pharmacol Rev 53:283-318.
16. Lin JT, Chen H, Wang D, Xiong L, Chen GB (2019) Nuclear-targeted p53 and DOX co-delivery of chitosan derivatives for cancer therapy in vitro and in vivo. Colloids Surf B 183:110440.
17. Oka M, Yoneda Y (2018) Importin α: functions as a nuclear transport factor and beyond. Proc Jpn Acad Ser B 94:259-274.

Figures

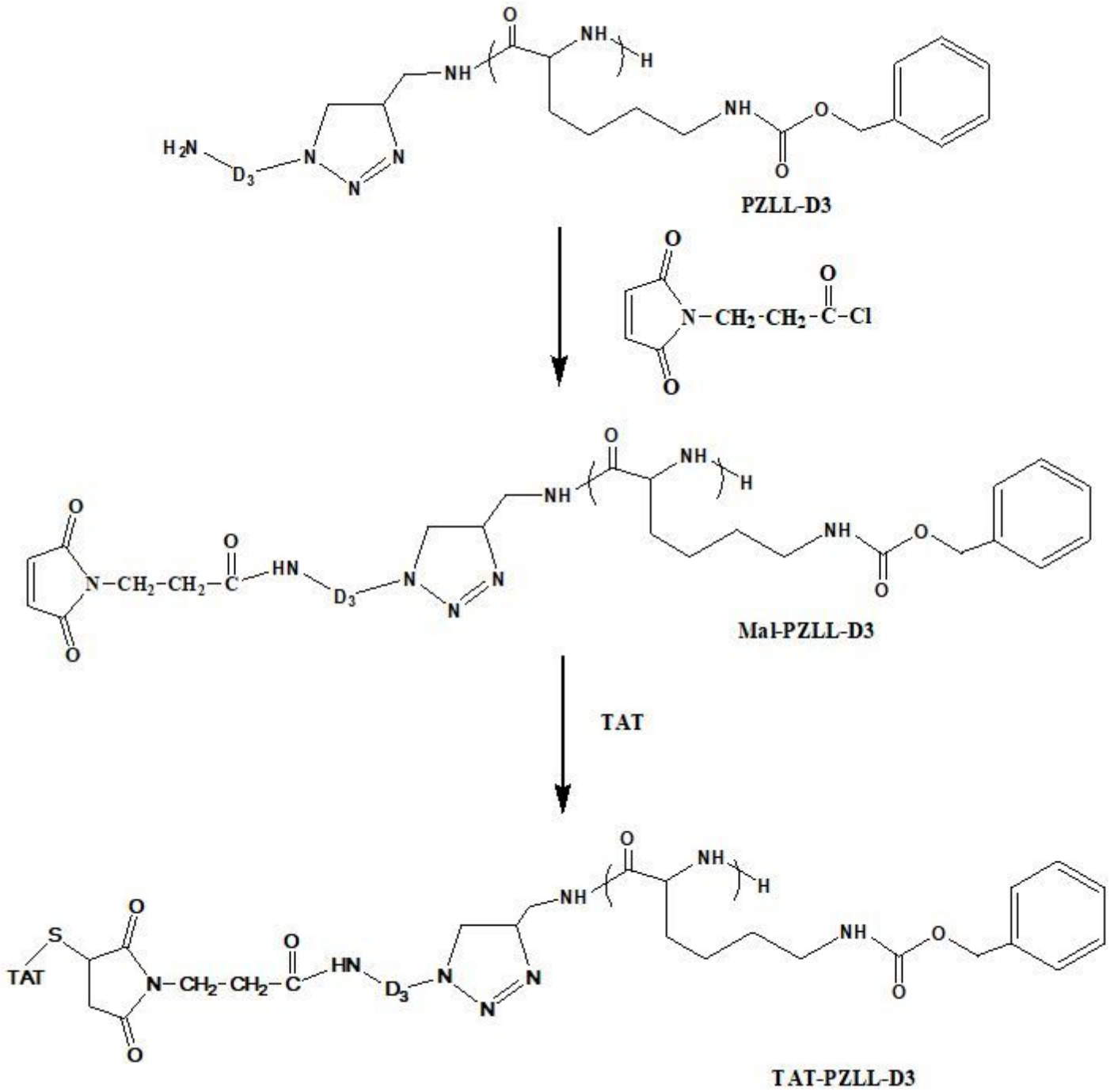

Figure 1

Synthesis of the TAT-PZLL-D3

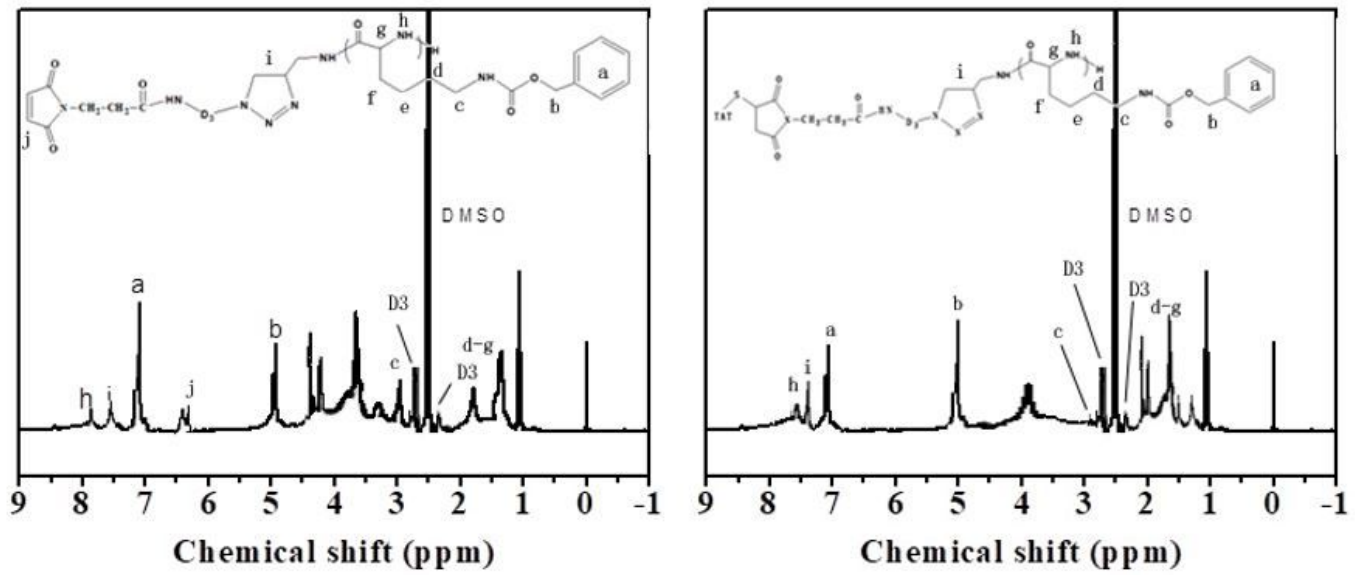

Figure 2

1H NMR spectrum of Mal-PZLL-D3 and TAT-PZLL-D3

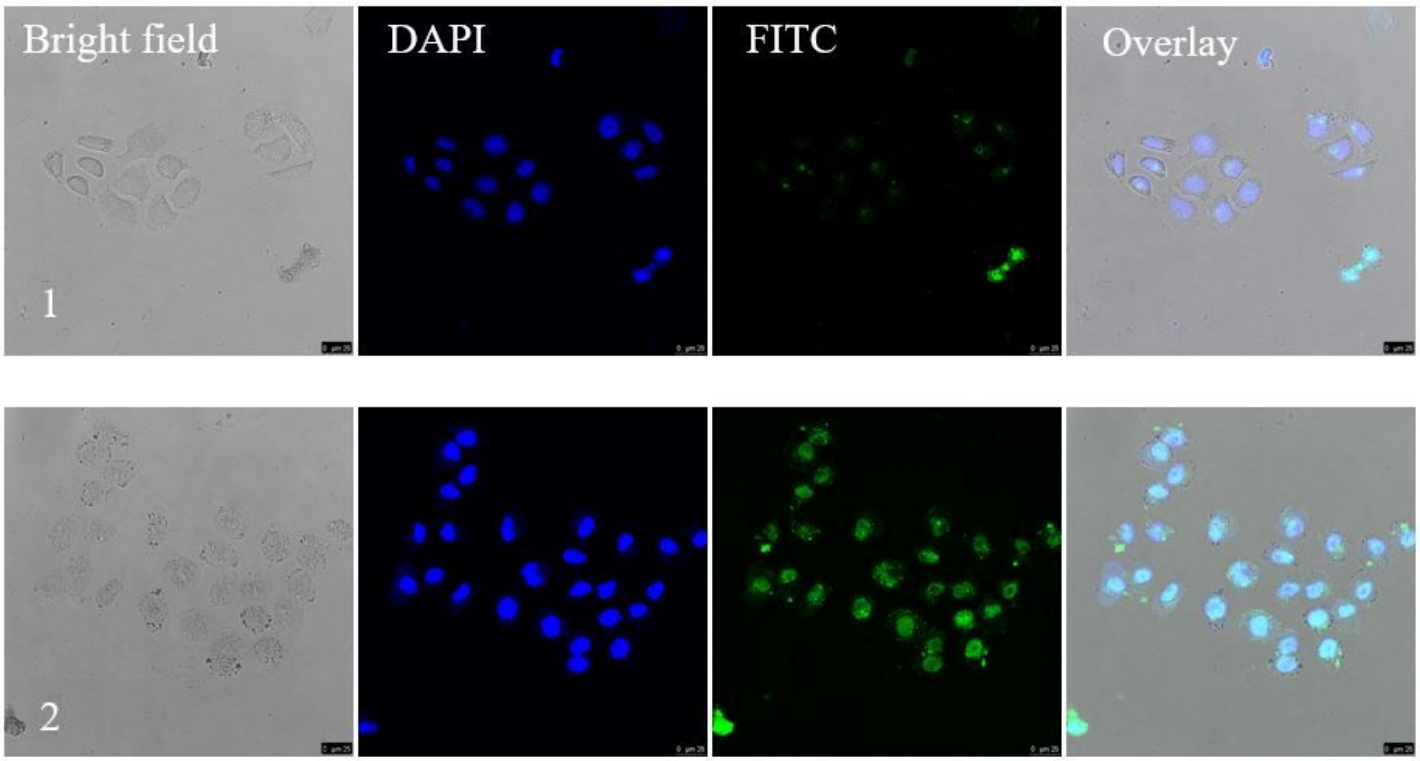

Figure 3

Location of an FITC marked carrier in A549 cells, recorded by CLSM. 1.PZLL-D3 2.TAT-PZLL-D3 The original magnification is 40×.

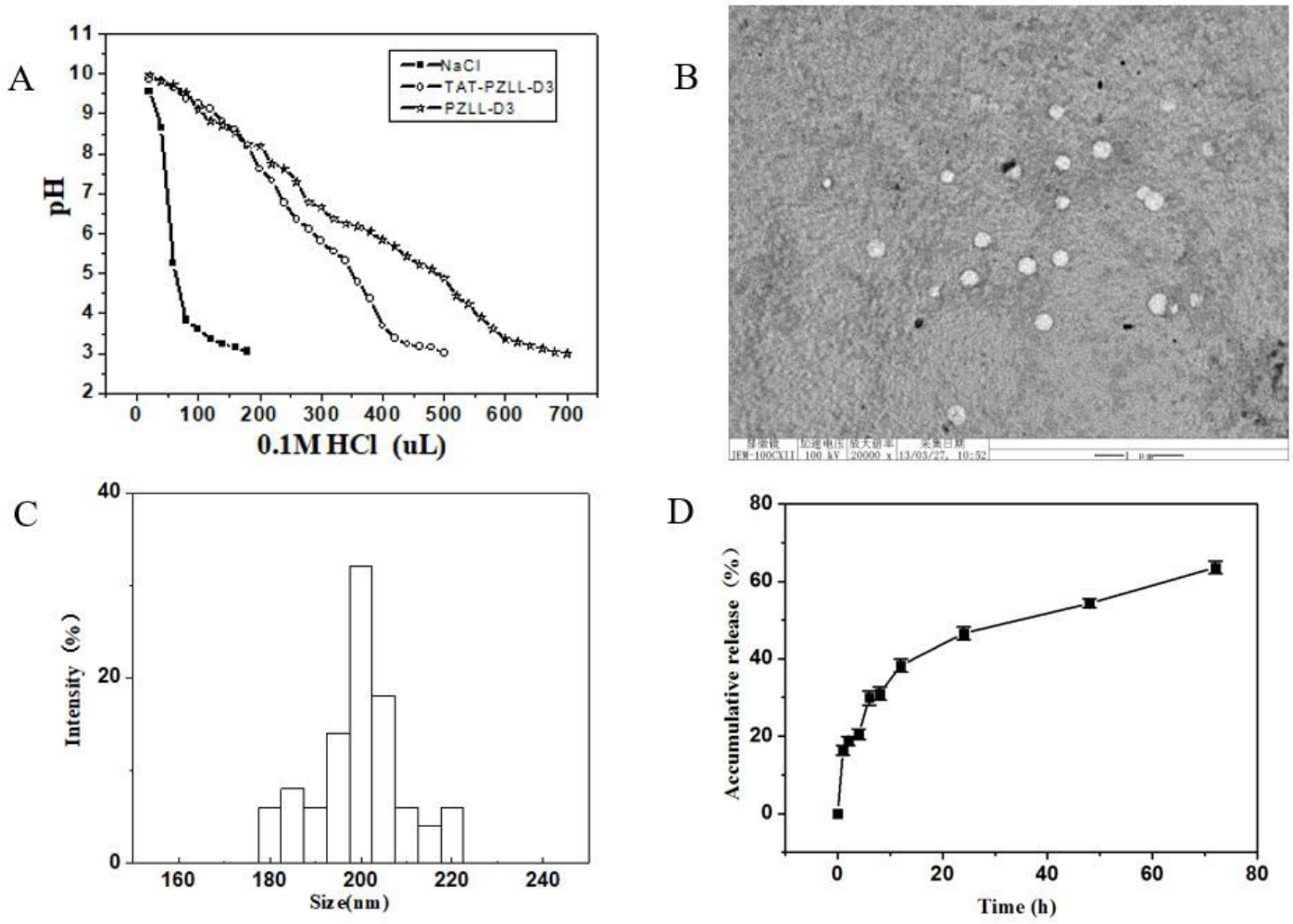

Figure 4

Buffer capacity of PZLL-D3 and TAT-PZLL-D3 at N/P=20. (A) Particle size distribution of TAT-PZLL-D3/p53 at N/P=20. (B) Typical TEM image of TAT-PZLL-D3/p53 at N/P=20. (C) Cumulative release of DOX from TAT-PZLL-D3 (D)

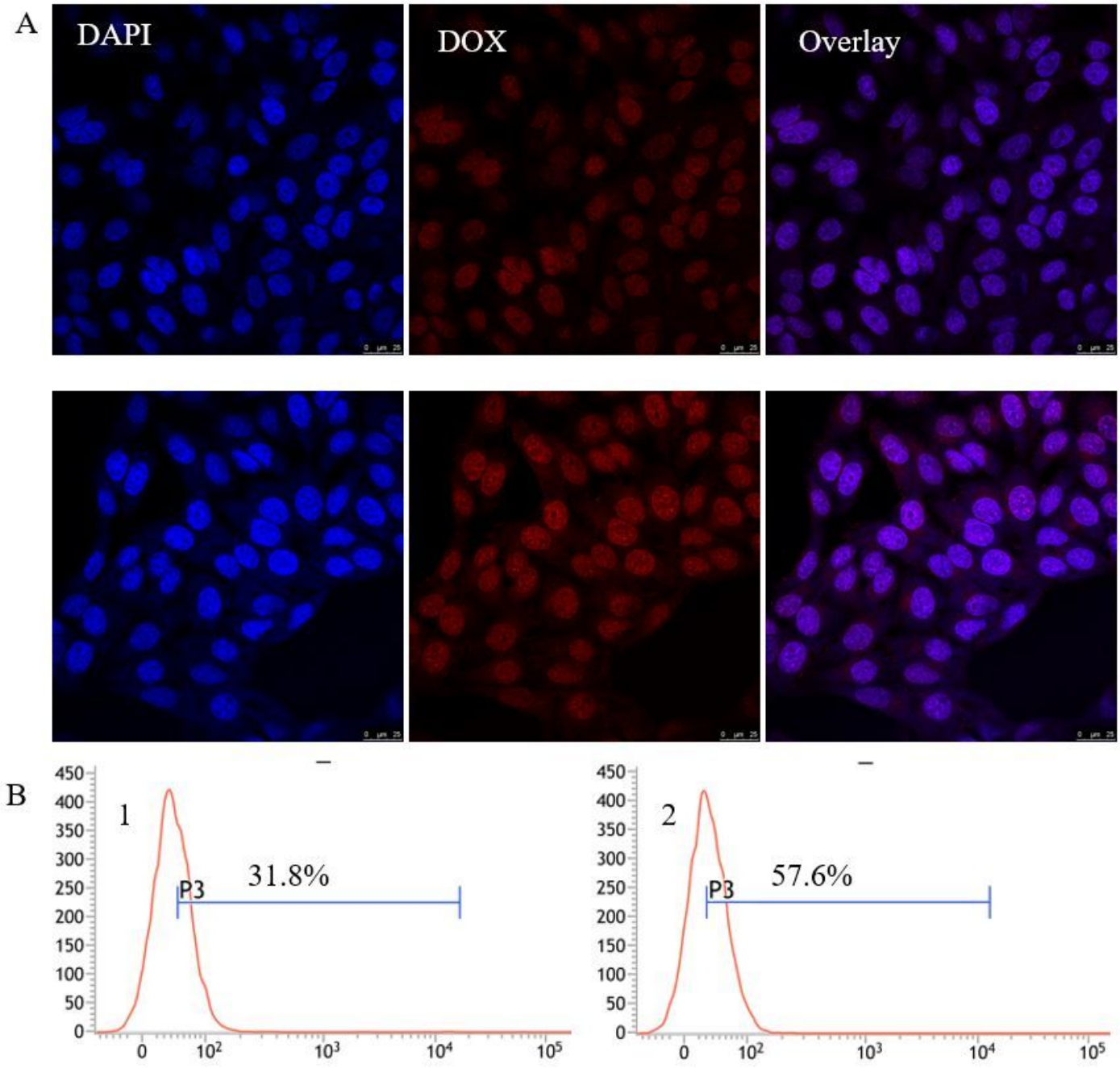

Figure 5

Representative CLSM images(A) and DOX-positive cell populations(B) measured by flow cytometry after A549 cell culture with 1. PZLL-D3/DOX 2. TAT-PZLL-D3/DOX (DOX=1μg per mL)

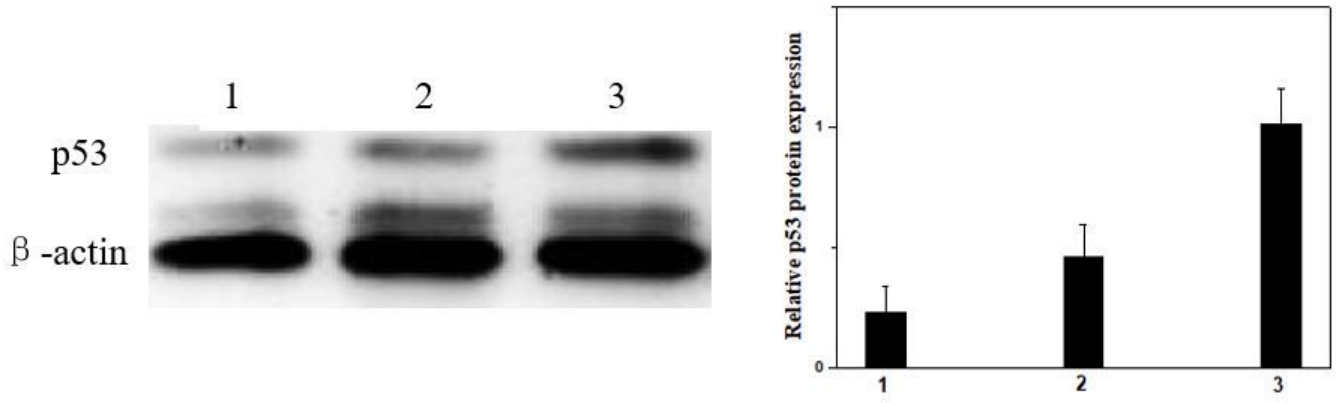

Figure 6

p53 protein expression determined by WB 1: TAT-PZLL-D3; 2: PZLL-D3/p53 (p53=2μg); 3:TAT-PZLL-D3/p53 (p53=2μg).The N/P ratio was fixed at 20.

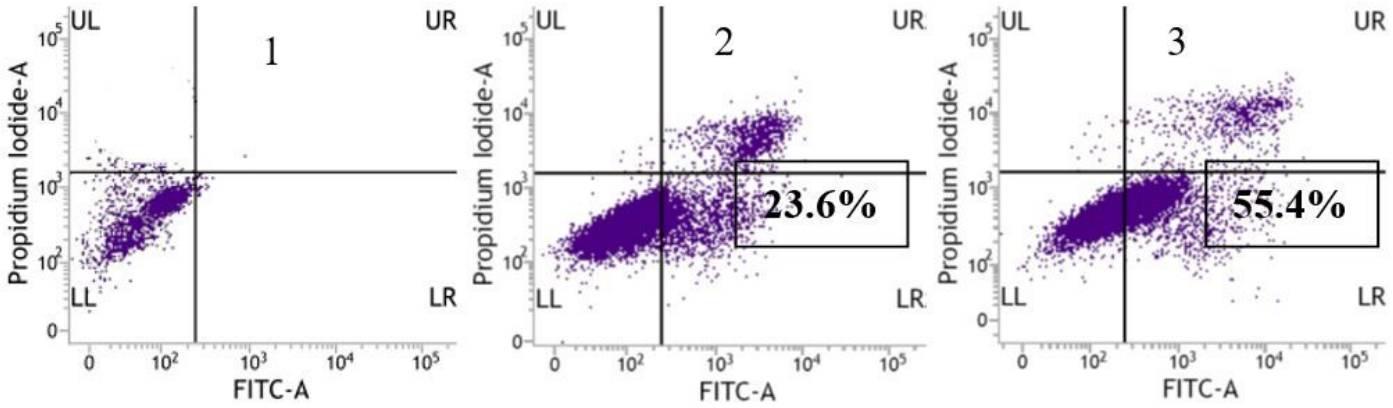

Figure 7

Apoptosis analysis by flow cytometry after incubation of A549 cells with various samples. 1: TAT-PZLL-D3; 2: PZLL-D3/p53/DOX (p53=2μg, DOX=1μg per mL); 3:TAT-PZLL-D3/p53/DOX (p53=2μg, DOX=1μg per mL).The N/P ratio was fixed at 20.

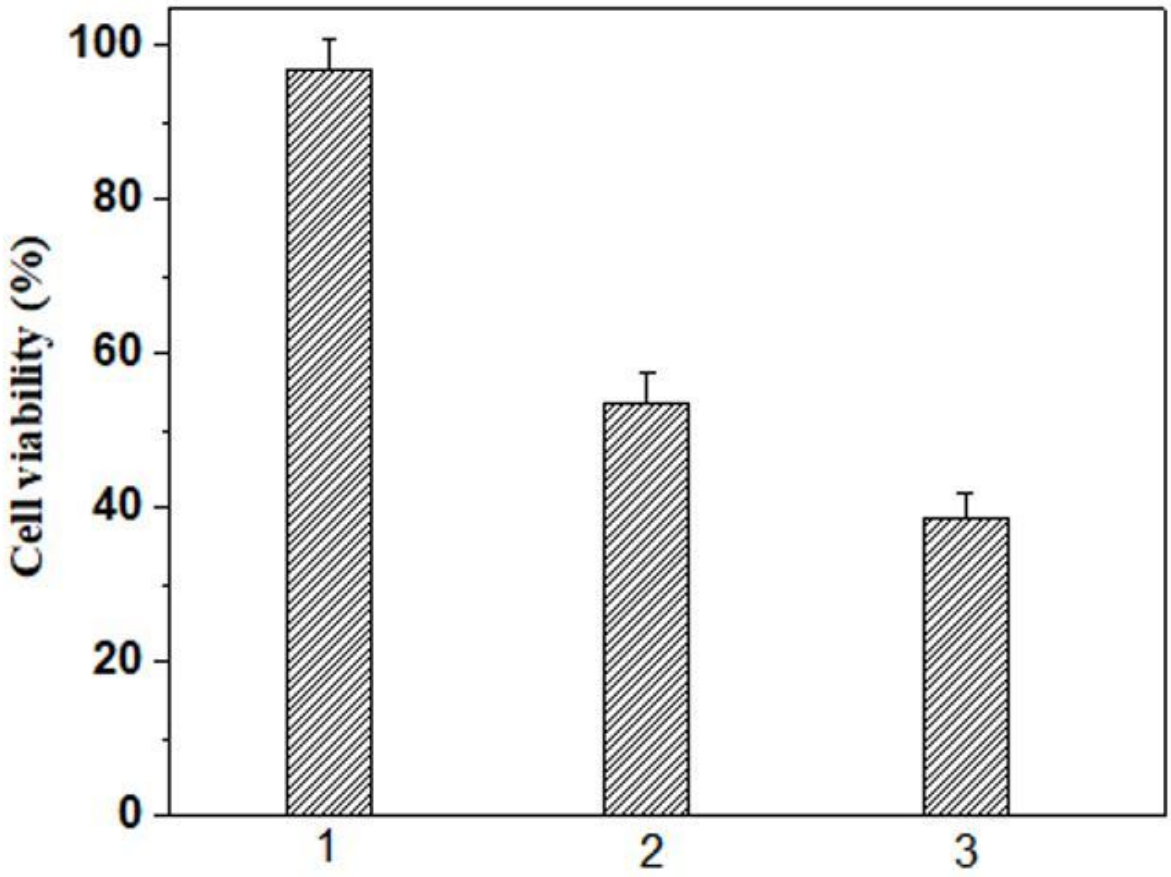

Figure 8

Cell viability after incubation of A549 cells with various samples. 1: TAT-PZLL-D3; 2: PZLL-D3/p53/DOX (p53=2μg, DOX=1μg per mL); 3:TAT- PZLL-D3/p53/DOX (p53=2μg, DOX=1μg per mL). The error bars represents standard deviation, n=6.